




¹⁸F-Fluoroethyl-tyrosine uptake is correlated with amino acid transport and neovascularization in treatment-naïve glioblastomas

Friederike Liesche¹ · Mathias Lukas^{2,3,4} · Christine Preibisch⁵ · Kuangyu Shi^{2,6} · Jürgen Schlegel¹ · Bernhard Meyer⁷ · Markus Schwaiger² · Claus Zimmer⁵ · Stefan Förster² · Jens Gempt⁷ · Thomas Pyka^{2,5} 

Received: 13 March 2019 / Accepted: 18 June 2019 / Published online: 9 July 2019
© Springer-Verlag GmbH Germany, part of Springer Nature 2019

Abstract

Purpose To investigate the in vivo correlation between ¹⁸F-fluoroethyl-tyrosine (¹⁸F-FET) uptake and amino acid transporter expression and vascularization in treatment-naïve glioblastomas.

Methods A total of 43 stereotactic biopsies were obtained from 13 patients with suspected glioblastoma prior to therapy. All patients underwent a dynamic ¹⁸F-FET PET/MRI scan before biopsy. Immunohistochemistry was performed using antibodies against SLC7A5 (amino acid transporter), MIB-1 (Ki67, proliferation), CD31 (vascularization) and CA-IX (hypoxia). The intensity of staining was correlated with ¹⁸F-FET uptake and the dynamic ¹⁸F-FET uptake slope at the biopsy target point.

Results In all patients, the final diagnosis was IDH-wildtype glioblastoma, WHO grade IV. Static ¹⁸F-FET uptake was significantly correlated with SLC7A5 staining ($r = 0.494$, $p = 0.001$). While the dynamic ¹⁸F-FET uptake slope did not show a significant correlation with amino acid transporter expression, it was significantly correlated with the number of CD31-positive vessels ($r = -0.350$, $p = 0.031$), which is line with earlier results linking ¹⁸F-FET kinetics with vascularization and perfusion. Besides, static ¹⁸F-FET uptake also showed correlations with CA-IX staining ($r = 0.394$, $p = 0.009$) and CD31 positivity ($r = 0.410$, $p = 0.006$). While the correlation between static ¹⁸F-FET uptake and SLC7A5 staining was confirmed as significant in multivariate analysis, this was not the case for the correlation with CD31 positivity, most likely because of the lower effect size and the relatively low number of samples. No significant correlation between ¹⁸F-FET uptake and Ki67 proliferation index was observed in our cohort.

Conclusion Our results support the findings of preclinical studies suggesting that specific ¹⁸F-FET uptake in glioblastomas is mediated by amino acid transporters. As proposed previously, dynamic ¹⁸F-FET parameters might be more influenced by perfusion and therefore related to properties of the tumour neovascularization.

Keywords ¹⁸F-Fluoroethyltyrosine PET · Glioblastoma · Histopathology · Immunohistochemistry · Amino acid transporter · Neovascularization

Jens Gempt and Thomas Pyka contributed equally to this work.

This article is part of the Topical Collection on Oncology – Brain

Electronic supplementary material The online version of this article (<https://doi.org/10.1007/s00259-019-04407-3>) contains supplementary material, which is available to authorized users.

✉ Thomas Pyka
thomas.pyka@tum.de

¹ Department of Neuropathology, Institute of Pathology, Technische Universität München, Trogerstraße 18, 81675 Munich, Germany

² Department of Nuclear Medicine, Klinikum rechts der Isar, Technische Universität München, Ismaninger Str. 22, 81675 Munich, Germany

³ Department of Nuclear Medicine, Charité-Universitätsmedizin Berlin, Charitéplatz 1, 10117 Berlin, Germany

⁴ Siemens Healthcare GmbH, Berlin, Germany

⁵ Department of Neuroradiology, Klinikum rechts der Isar, Technische Universität München, Ismaninger Str. 22, 81675 Munich, Germany

⁶ Department of Nuclear Medicine, Universität Bern, Hochschulstraße 6, 3012 Bern, Switzerland

⁷ Department of Neurosurgery, Klinikum rechts der Isar, Technische Universität München, Ismaninger Str. 22, 81675 Munich, Germany

Introduction

Although ^{18}F -fluoroethyl-tyrosine (^{18}F -FET) has become the most important PET radiotracer for the examination of brain tumours in Europe [1], the exact uptake mechanism in vivo is still a matter of debate. Preclinical experiments suggest that amino acid transporters, particularly the large neutral amino acid transporter 1 (LAT1/SCL7A5), might play a crucial role [2]. In addition, “fast” ^{18}F -FET kinetics, i.e. rapid uptake and washout on dynamic PET scans, which can be measured as early time-to-peak and negative late slope values in the time–activity curves, have shown some specificity for high-grade glioma tissue, for reasons yet unknown [3–5]. However, a systematic evaluation of the spatial correlation between dynamic ^{18}F -FET PET and amino acid transporter expression in human gliomas has not yet been performed. In this prospective study, we investigated the relationship between static ^{18}F -FET uptake and dynamic uptake behaviour and histological markers, including SCL7A5 expression and vascularization, using stereotactic biopsies in patients with untreated glioblastoma.

Materials and methods

Patients and imaging protocol

From February 2013 to July 2016, participation in this prospective study was offered to patients with suspected high-grade glioma. All patients underwent dynamic ^{18}F -FET PET scans on a hybrid PET/MR system (Biograph mMR; Siemens Healthcare, Malvern, PA) before surgery. To achieve standardized metabolic conditions, patients had to fast for a minimum of 6 h. After intravenous injection of a target dose of 190 MBq *O*-(2- ^{18}F -fluoroethyl)-L-tyrosine, FET PET acquisitions were performed for 40 min. From the list-mode PET data, static images at 30–40 min after injection and dynamic images (20×3 s, 2×5 s, 2×10 s, 2×20 s, 2×30 s, 2×60 s, 2×120 s, 2×180 and 6×300 s) were reconstructed using 3D OSEM into 192×192 matrices, resulting in an isotropic voxel size of 1.16 mm^3 . Tumour-to-background ratios (TBR) were calculated by normalizing to contralateral healthy-appearing brain tissue. From the dynamic images, the linear slope between 15 and 40 min after injection was calculated on the time–activity curves as described previously [5] (see also Fig. 2). 3D T2-weighted fluid attenuated inversion recovery (FLAIR), T2*-weighted gradient echo and contrast enhanced T1-weighted magnetization prepared rapid acquisition gradient echo (MPRAGE) images were acquired for morphological correlation. Attenuation and scatter correction were performed using attenuation maps based on a segmentation approach [6].

VOI definition and stereotactic biopsies

Spherical volumes of interest (VOI) of 1 cm diameter were defined on the PET images in consensus with the operating neurosurgeons to include spots of both high and low static FET uptake as well as areas of different dynamic uptake behaviour, therefore also including spots with intermediate FET uptake. Morphological MRI correlation was performed to ensure all VOIs were located in solid tumour and did not include necrotic areas. Using a cranial navigation system (Varioguide, Brainlab AG, Munich, Germany; stereotactic accuracy approximately 3 mm), several biopsies per patient were obtained and sent in 10% buffered formalin to the Department of Neuropathology for histological evaluation.

Immunohistochemistry

CD31 and Mib-1 immunohistochemistry was performed on formalin-fixed paraffin-embedded tissue using a fully automated staining system (Ventana BenchMark ULTRA; Ventana Medical Systems; Tucson, AZ) with pretreatment in pH 8.4 buffer at 95°C and H_2O_2 , and then charging with monoclonal IgG mouse anti-CD31 antibody (Clone JC70A; DakoCytomation Denmark A/S, Denmark; dilution 1:50) or IgG rabbit anti-Mib1 (Thermo Fisher Scientific, UK; dilution 1:100). For antibody detection, an OptiView DAB IHC detection kit (Ventana Medical Systems) was used. CA-IX and SLC7A5 immunohistochemistry was performed manually, starting with pretreatment of the sections in pH 6.0 citrate buffer at 95°C and H_2O_2 , followed by incubation with monoclonal IgG rabbit anti-CA-IX antibody (Clone D10C10; Cell Signaling Technology, USA; dilution 1:100) or polyclonal rabbit anti-SLC7A5 (abcam, UK; dilution 1:150), and then with biotinylated secondary anti-rabbit IgG antibody (Vector Laboratories, USA; 1:400). ABC reagent (Vector Laboratories) and then diaminobenzidine (Dako, USA) were applied. All immunostained sections were counterstained with haematoxylin and positive controls were included for quality assurance.

Staining evaluation

Two experienced neuropathologists (F.L., J.S.), not aware of the results of the PET analysis, evaluated the immunohistochemical staining. A proliferation index was specified as the percentage of Mib-1-positive cells (Ki67 index). CA-IX and SLC7 immunohistochemistry were scaled from 0 to 3, with 0 indicating no protein expression. For evaluation of the expression of CA-IX and SCL7A5 proteins, the proportions of stained cells plus staining intensity were taken into account, leading to a value from 1 for sparse protein expression to 3 for strong and broadly distributed immunoreactivity. CD31 immunostaining was scaled from 0 to 3 by evaluation of the

number of vessels in relation to the gross tumour area (see Supplementary Fig. 1 for examples of the different histological scores). A final diagnosis was obtained from the tumour material gathered (biopsies plus surgical material), taking into account features of mitotic activity, necrosis and neovascularization, and IDH status.

Statistical analysis

All statistical analyses were performed using SPSS 24 (IBM Corp., Armonk, NY, USA). Correlations between FET PET and histological parameters were evaluated using Spearman's correlation coefficient. In addition, logistic regression with dichotomization of histological parameters was used for multivariate analysis. Values of $p < 0.05$ were considered statistically significant.

Results

A total of 43 stereotactic biopsies were obtained from 13 patients (68 ± 8 years, six women, seven men; one to five biopsies per patient). In all patients, the final diagnosis was IDH-wildtype glioblastoma, WHO grade IV.

The mean static ^{18}F -FET uptake, expressed as TBR, in the biopsy VOI was 2.27 (0.97–5.14), the mean slope was 0.09

times the standardized uptake value (SUV) per hour (range -4.04 – 2.03). The mean values for SLC7A5 staining, CD31-positive vessels and CA-IX 1.14 staining were 1.58 (range 0–3), 0.98 (range 0–3) and 1.14 (range 0–3), respectively. Static ^{18}F -FET uptake showed a significant correlation with SLC7A5 staining ($r = 0.494$, $p = 0.001$; an example is shown in Fig. 1). Static ^{18}F -FET uptake also showed a significant correlation with hypoxia expressed in terms of CA-IX staining ($r = 0.394$, $p = 0.009$). While the dynamic ^{18}F -FET slope showed no significant correlation with either SLC7A5 staining ($r = 0.046$, $p = 0.785$) or CA-IX staining ($r = 0.115$, $p = 0.493$), it did show a significant correlation with a higher number of CD31-positive vessels ($r = -0.350$, $p = 0.031$; an example is shown in Fig. 2). Static ^{18}F -FET uptake also showed a significant correlation with CD31 staining ($r = 0.410$, $p = 0.006$, but ^{18}F -FET uptake showed no significant correlation with the Ki67 proliferation index ($r = 0.049$, $p = 0.770$, for dynamic uptake; $r = 0.240$, $p = 0.121$, for static uptake). In addition, logistic regression was performed. While the correlation between static ^{18}F -FET uptake and LAT1 expression was confirmed in the multivariate analysis ($p = 0.012$), the relationship between ^{18}F -FET uptake (both static and dynamic) and CD31 expression failed to reach significance ($p = 0.053$ and $p = 0.472$, respectively). The results of the statistical analysis are presented in Table 1.

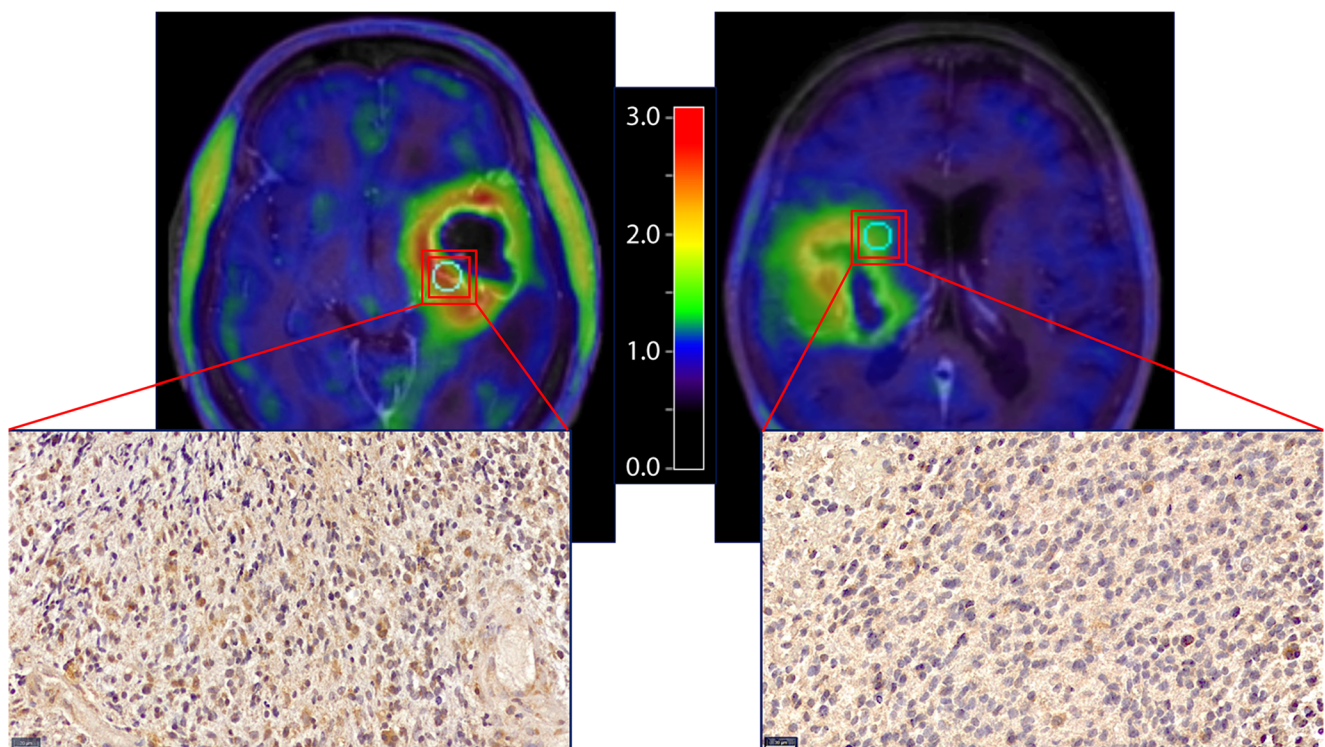


Fig. 1 Histopathological correlation between static FET PET and amino acid transporter expression in two patients with IDH-wildtype glioblastoma. *Left*: Strong immunoreactivity for SLC7A in a high

number of tumour cells (score 3; scale bar 20 μm); FET TBR is 2.8. *Right*: Moderate SLC7A immunoreactivity in several tumour cells (score 2; scale bar 20 μm); FET TBR is 1.6

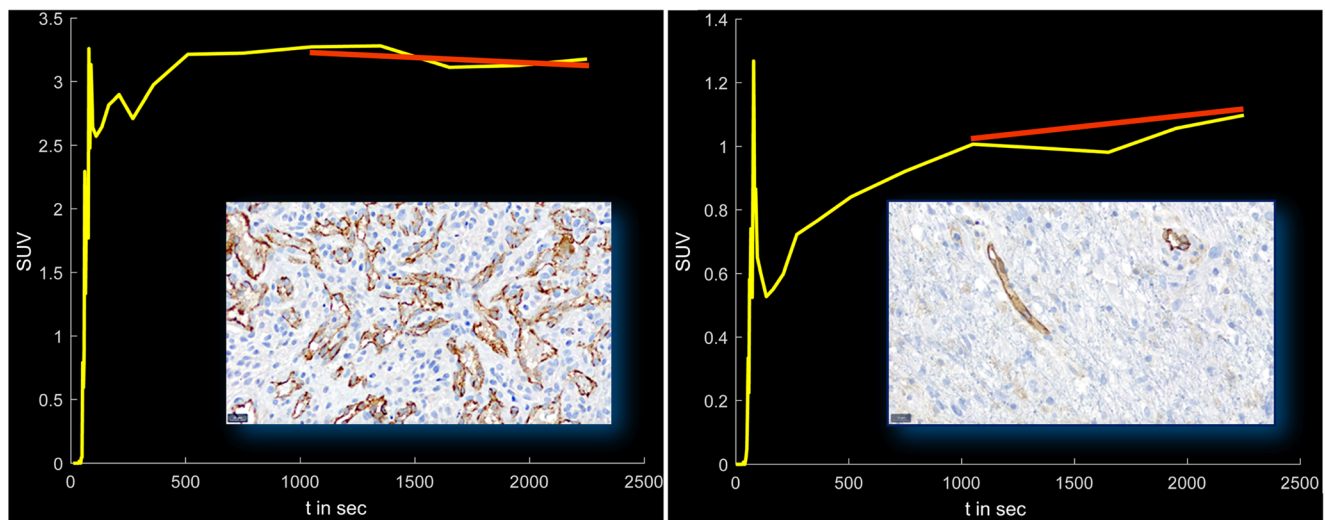


Fig. 2 Histopathological correlation between FET PET and neovascularization in two patients with IDH-wildtype glioblastoma. *Left*: CD31 immunoreactivity indicates a high number of vascular proliferations (score 3; scale bar 20 μ m). The FET time-activity-curve shows “fast” FET kinetics with an early peak, an uptake plateau and

subsequent washout, corresponding to a slightly negative slope value (slope shown in red). *Right*: CD31 immunoreactivity shows only a few vessels (score 1; scale bar 20 μ m). The FET time-activity curve shows a steady increase in FET uptake, corresponding to a positive slope value

Discussion

For many years, there has been a constant debate about the possible ^{18}F -FET uptake mechanism in gliomas. ^{18}F -FET uptake in most tumours is considerable, although there is only minor ^{18}F -FET degradation and no relevant involvement in protein synthesis in the human body [7]. Subtypes of system L-amino acid transporters have been proposed as possible transport pathways for ^{18}F -FET. Recently, Habermeier et al. demonstrated that the Na^+ -independent amino acid antiporter LAT1, also known as SLC7A5, might be responsible for the intracellular accumulation of ^{18}F -FET in LN229 human glioblastoma cells [2]. SLC7A5 is highly expressed in gliomas, probably helping to meet the increased amino acid demand of proliferating and infiltrating tumour cells, and elevated expression is associated with higher tumour grade, e.g. glioblastoma [8]. The results of Habermeier et al. are in contrast to those of another group indicating that ^{18}F -FET is only poorly transported by LAT1 in *Xenopus laevis* oocytes [9]. Our results, however, support an association between SCL7A5

expression and ^{18}F -FET uptake in human glioblastomas, and might therefore explain the relative specificity of ^{18}F -FET PET for glioma tissue due to upregulation of amino acid transporters. We used an in vivo approach with stereotactically guided biopsies, and demonstrated a significant correlation between ^{18}F -FET uptake on static images and SLC7A5 protein expression as measured by immunohistochemistry in tissue samples of IDH-wildtype glioblastomas. Additionally, the confirmation of LAT1 as the key to specific ^{18}F -FET uptake might enhance our understanding of interindividual and intraindividual variations on ^{18}F -FET PET imaging, e.g. due to nutritional factors. The emergence of LAT1 as a possible target for biological tumour therapies is another aspect, which might foster the use of ^{18}F -FET PET for therapy monitoring in the future.

In this work, we showed a significant correlation between the dynamic ^{18}F -FET uptake slope and the amount of neovascularization, but no correlation with LAT1 expression. “Fast” ^{18}F -FET kinetics with both rapid tracer uptake and wash-out have been associated with the

Table 1 Spearman’s correlation coefficients and multivariate logistic regression results for FET PET parameters and histological markers obtained from stereotactic biopsies

		Ki67	CA IX	SLC7A	CD31
FET slope	<i>r</i>	−0.049	−0.115	0.046	−0.350
	<i>p</i>	0.770	0.493	0.785	0.031
	<i>p</i> (multivariate analysis)	—	0.737	0.839	0.472
FET tumour-to-background ratio	<i>r</i>	0.240	0.394	0.494	0.410
	<i>p</i>	0.121	0.009	0.001	0.006
	<i>p</i> (multivariate analysis)	—	0.072	0.014	0.053

Values indicating significant correlations are printed in bold

presence of high-grade glioma tissue [4], and have already been demonstrated to be related to vascular imaging markers such as cerebral blood volume [10], and this is supported by the results of studies using kinetic multicompartiment models [11]. These results can be summarized under the hypothesis that FET kinetic parameters are more likely to be associated with characteristics of tumour vascularization than with amino acid transport itself. It is not surprising that static FET uptake also showed a correlation with the degree of vascularization, either by indicating hot spots of higher malignancy or by the perfusion dependence of the FET signal itself. However, while the correlation between static FET uptake and LAT1 expression was confirmed in the multivariate regression analysis, the correlations with vascularization did not achieve significance in the multivariate statistics, most likely due to the weaker effect and the low number of patients and biopsies in our study.

In glioblastomas, hypoxia is associated with aggressiveness and a poor prognosis [12]. Our results showed a correlation between static ^{18}F -FET uptake and CA-IX expression, which indicates that ^{18}F -FET uptake has a certain dependence on hypoxia, although we cannot yet provide a conclusive explanation for this phenomenon. Finally, we did not find a correlation between ^{18}F -FET uptake and proliferation as represented by the Ki67 index, confirming the findings of previous studies on this matter [13]. This also provides an indication that the significant correlations described cannot be considered as purely coincidental.

In this study, we tried to mitigate the impact of intratumoural heterogeneity, an important feature of glioblastomas, by spatial coregistration of ^{18}F -FET PET images with stereotactic biopsies. However, we cannot exclude the possibility that heterogeneity on a smaller scale, which is difficult to detect on PET due to its limited resolution, might still have affected our analysis.

Conclusion

The results of this prospective study support the hypothesis that ^{18}F -FET uptake is associated with the expression of LAT1 (SCL7A5) in human glioblastomas. On the other hand, and in line with the findings of previous studies, dynamic ^{18}F -FET uptake seems to be more correlated with the neo-vascularization of the tumour.

Funding This study was supported by funding from the German Research Foundation DFG (grants to C.P., S.F. and T.P.; FO 886/1-1, PR 1039/4-1).

Compliance with ethical standards

Conflicts of interest B.M. and J.G. report personal fees from Brain Lab AG outside the submitted work. C.Z. has served on scientific advisory boards for Philips N.V. and Bayer Schering AG. All the other authors declare that they have no conflicts of interest.

Ethical approval All procedures performed in studies involving human participants were approved by the Ethics Committee of the Medical Faculty of the Technische Universität München (vote 5547/12) and were in accordance with the principles of the 1964 Declaration of Helsinki and its later amendments.

Informed consent Informed consent was obtained from all individual participants included in the study.

References

1. Albert NL, Weller M, Suchorska B, Galldiks N, Soffietti R, Kim MM, et al. Response Assessment in Neuro-Oncology working group and European Association for Neuro-Oncology recommendations for the clinical use of PET imaging in gliomas. *Neuro Oncol*. 2016;18:1199–208. <https://doi.org/10.1093/neuonc/nov058>.
2. Habemeier A, Graf J, Sandhofer BF, Boissel JP, Roesch F, Closs EI. System L amino acid transporter LAT1 accumulates O-(2-fluoroethyl)-L-tyrosine (FET). *Amino Acids*. 2015;47:335–44. <https://doi.org/10.1007/s00726-014-1863-3>.
3. Kunz M, Thon N, Eigenbrod S, Hartmann C, Egensperger R, Herms J, et al. Hot spots in dynamic (18)F-FET-PET delineate malignant tumor parts within suspected WHO grade II gliomas. *Neuro Oncol*. 2011;13:307–16. <https://doi.org/10.1093/neuonc/noq196>.
4. Rohrich M, Huang K, Schrimpf D, Albert NL, Hielscher T, von Deimling A, et al. Integrated analysis of dynamic FET PET/CT parameters, histology, and methylation profiling of 44 gliomas. *Eur J Nucl Med Mol Imaging*. 2018;45:1573–84. <https://doi.org/10.1007/s00259-018-4009-0>.
5. Vomacka L, Unterrainer M, Holzgreve A, Mille E, Gosewisch A, Brosch J, et al. Voxel-wise analysis of dynamic (18)F-FET PET: a novel approach for non-invasive glioma characterisation. *EJNMMI Res*. 2018;8:91. <https://doi.org/10.1186/s13550-018-0444-y>.
6. Izquierdo-Garcia D, Hansen AE, Förster S, Benoit D, Schachoff S, Fürst S, et al. An SPM8-based approach for attenuation correction combining segmentation and nonrigid template formation: application to simultaneous PET/MR brain imaging. *J Nucl Med*. 2014;55:1825–30. <https://doi.org/10.2967/jnumed.113.136341>.
7. Pauleit D, Floeth F, Herzog H, Hamacher K, Tellmann L, Müller HW, et al. Whole-body distribution and dosimetry of O-(2-[18F]fluoroethyl)-L-tyrosine. *Eur J Nucl Med Mol Imaging*. 2003;30:519–24. <https://doi.org/10.1007/s00259-003-1118-0>.
8. Nawashiro H, Otani N, Shinomiya N, Fukui S, Ooigawa H, Shima K, et al. L-type amino acid transporter 1 as a potential molecular target in human astrocytic tumors. *Int J Cancer*. 2006;119:484–92. <https://doi.org/10.1002/ijc.21866>.
9. Lahouette T, Caveliers V, Camargo SM, Franca R, Ramadan T, Veljkovic E, et al. SPECT and PET amino acid tracer influx via system L (h4F2hc-hLAT1) and its transstimulation. *J Nucl Med*. 2004;45:1591–6.
10. Gottler J, Lukas M, Kluge A, Kaczmarz S, Gempt J, Ringel F, et al. Intra-lesional spatial correlation of static and dynamic FET-PET parameters with MRI-based cerebral blood volume in patients with

- untreated glioma. *Eur J Nucl Med Mol Imaging*. 2017;44:392–7. <https://doi.org/10.1007/s00259-016-3585-0>.
11. Debus C, Afshar-Oromieh A, Floca R, Ingris M, Knoll M, Debus J, et al. Feasibility and robustness of dynamic (18)F-FET PET based tracer kinetic models applied to patients with recurrent high-grade glioma prior to carbon ion irradiation. *Sci Rep*. 2018;8:14760. <https://doi.org/10.1038/s41598-018-33034-5>.
 12. Evans SM, Jenkins KW, Chen HI, Jenkins WT, Judy KD, Hwang WT, et al. The relationship among hypoxia, proliferation, and outcome in patients with de novo glioblastoma: a pilot study. *Transl Oncol*. 2010;3:160–9.
 13. Stockhammer F, Plotkin M, Amthauer H, van Landeghem FK, Woiciechowsky C. Correlation of F-18-fluoro-ethyl-tyrosin uptake with vascular and cell density in non-contrast-enhancing gliomas. *J Neurooncol*. 2008;88:205–10. <https://doi.org/10.1007/s11060-008-9551-3>.

Publisher's note Springer Nature remains neutral with regard to jurisdictional claims in published maps and institutional affiliations.